



**University of
Zurich^{UZH}**

**Zurich Open Repository and
Archive**

University of Zurich
University Library
Strickhofstrasse 39
CH-8057 Zurich
www.zora.uzh.ch

Year: 2015

Intratumor heterogeneity in hepatocellular carcinoma

Friemel, Juliane ; Rechsteiner, Markus Peter ; Frick, Lukas ; Boehm, Friederike ; Struckmann, Kirsten ; Sigg, Michele ; Moch, Holger ; Heikenwaelder, Mathias ; Weber, Achim

Abstract: Purpose: Morphologic intratumor heterogeneity is well known to exist in hepatocellular carcinoma (HCC) but very few systematic analyses of this phenomenon have been performed. The aim of this study was to comprehensively characterize morphological intratumor heterogeneity in HCC. Also taken into account were well-known immunohistochemical markers and molecular changes in liver cells that are considered in proposed classifications of liver cell neoplasms or discussed as molecular therapeutic targets. Experimental Design: In HCC of 23 patients without medical pretreatment, a total of 120 tumor areas were defined. Analyzed were cell and tissue morphology, expression of the liver cell markers CK7, CD44, AFP, EpCAM and glutamine synthetase along with mutations of TP53 and CTNNB1, assayed by both Sanger and next generation sequencing. Results: Overall, intratumor heterogeneity was detectable in the majority of HCC cases (20/23, 87%). Heterogeneity solely on the level of morphology was found in 6/23 cases (26%), morphological heterogeneity combined with immunohistochemical heterogeneity in 9/23 cases (39%), and heterogeneity with respect to morphology, immunohistochemistry and mutational status of TP53 and CTNNB1 in 5/23 cases (22%). Conclusions: Our findings demonstrate that intratumor heterogeneity represents a challenge for the establishment of a robust HCC classification and may contribute to treatment failure and drug resistance in many cases of HCC.

DOI: <https://doi.org/10.1158/1078-0432.CCR-14-0122>

Posted at the Zurich Open Repository and Archive, University of Zurich

ZORA URL: <https://doi.org/10.5167/uzh-99957>

Journal Article

Accepted Version

Originally published at:

Friemel, Juliane; Rechsteiner, Markus Peter; Frick, Lukas; Boehm, Friederike; Struckmann, Kirsten; Sigg, Michele; Moch, Holger; Heikenwaelder, Mathias; Weber, Achim (2015). Intratumor heterogeneity in hepatocellular carcinoma. *Clinical Cancer Research*, 21(8):1951-1961.

DOI: <https://doi.org/10.1158/1078-0432.CCR-14-0122>

Clinical Cancer Research



Intratumor heterogeneity in hepatocellular carcinoma

Juliane Friemel, Markus Peter Rechsteiner, Lukas Frick, et al.

Clin Cancer Res Published OnlineFirst September 23, 2014.

Updated version	Access the most recent version of this article at: doi: 10.1158/1078-0432.CCR-14-0122
Supplementary Material	Access the most recent supplemental material at: http://clincancerres.aacrjournals.org/content/suppl/2014/09/24/1078-0432.CCR-14-0122.DC1.html
Author Manuscript	Author manuscripts have been peer reviewed and accepted for publication but have not yet been edited.

E-mail alerts	Sign up to receive free email-alerts related to this article or journal.
Reprints and Subscriptions	To order reprints of this article or to subscribe to the journal, contact the AACR Publications Department at pubs@aacr.org .
Permissions	To request permission to re-use all or part of this article, contact the AACR Publications Department at permissions@aacr.org .

Intratumor heterogeneity in hepatocellular carcinoma

Running title: Implications for tumor classifications and targeted therapies

Juliane Friemel^{1,2}, Markus Rechsteiner¹, Lukas Frick¹, Friederike Böhm¹, Kirsten Struckmann¹, Michèle Sigg¹, Holger Moch¹, Mathias Heikenwalder^{1,3}, Achim Weber¹

1 Institute of Surgical Pathology, University Hospital Zurich, Zurich, Switzerland

2 Leibniz Institute for Prevention Research and Epidemiology, BIPS GmbH, Bremen, Germany

3 Institute of Virology, Technische Universität München (TUM) and Helmholtz Zentrum München für Gesundheit und Umwelt (HMGU), Germany

Key words: hepatocellular carcinoma, intratumor heterogeneity, multiregional sequencing

Financial support: This work was supported by the following grants: A grant from the Theiler-Haag Stiftung, Zurich to AW and LF. Grants from the Krebsliga Schweiz (Oncosuisse), Promedica Stiftung, the „Julius Müller Stiftung“, and from the “Kurt and Senta Herrmann Stiftung”, Vaduz, Lichtenstein to AW and MH. MH is also supported by an ERC Starting grant “LiverCancerMechanism”, the Hofschneider foundation and the Sonderforschungsbereich SFBTR36.

abbreviations: AFP: α -fetoprotein, bp: base pair, CD: cluster of differentiation, CK: cytokeratin, CTNNB1: β -catenin, EpCAM: epithelial adhesion molecule, GS: glutamine synthetase, HCA: hepatocellular adenoma, HCC: hepatocellular carcinoma, PCR: polymerase chain reaction, SD: standard deviation, TP53: tumor protein 53, TACE: transcatheter arterial chemoembolization, Wnt: wingless Int-1.

The authors disclose no conflict of interests.

Statement of translational relevance

In the era of targeted molecular therapies, intratumor heterogeneity is an emerging challenge to successful cancer therapy since it may result in evasion of therapy of distinct cell subpopulations or in development of therapy resistance as an adaptive phenomenon to specific inhibiting therapies. Therefore, investigating the frequency of and comprehensively characterizing intratumor heterogeneity is crucial. In hepatocellular carcinoma (HCC), it is known that tumors can display intratumoral heterogeneous morphology and histological differentiation grades. In our study we aimed to make a link between morphological intratumor heterogeneity, immune phenotypes (CK7, CD44, AFP, EpCAM, glutamine synthetase) and genetic heterogeneity of the two most important driver mutations in HCC (*CTNNB1* and *TP53*), of which β -catenin (*CTNNB1*) represents a potential therapeutic target. We used multiregional sequencing, supplementing Sanger sequencing with next generation sequencing which added a high level of accuracy to our analyses. Our results illustrate that intratumor heterogeneity is a frequent finding in HCC, which has implications not only for targeted therapies but also for establishing a robust HCC classification in daily clinical practice.

correspondence:

Achim Weber, MD

Institute of Surgical Pathology, University Hospital

Schmelzbergstrasse 12, CH-8091 Zurich, Switzerland

phone:++ 41 (0) 44 255 2781

fax:++ 41 (0) 44 255 4416

e-mail: achim.weber@usz.ch

Abstract

Purpose: Morphologic intratumor heterogeneity is well known to exist in hepatocellular carcinoma (HCC) but very few systematic analyses of this phenomenon have been performed. The aim of this study was to comprehensively characterize morphological intratumor heterogeneity in HCC. Also taken into account were well-known immunohistochemical markers and molecular changes in liver cells that are considered in proposed classifications of liver cell neoplasms or discussed as molecular therapeutic targets. **Experimental design:** In HCC of 23 patients without medical pretreatment, a total of 120 tumor areas were defined. Analyzed were cell and tissue morphology, expression of the liver cell markers CK7, CD44, AFP, EpCAM and glutamine synthetase along with mutations of *TP53* and *CTNNB1*, assayed by both Sanger and next generation sequencing. **Results:** Overall, intratumor heterogeneity was detectable in the majority of HCC cases (20/23, 87%). Heterogeneity solely on the level of morphology was found in 6/23 cases (26%), morphological heterogeneity combined with immunohistochemical heterogeneity in 9/23 cases (39%), and heterogeneity with respect to morphology, immunohistochemistry and mutational status of *TP53* and *CTNNB1* in 5/23 cases (22%). **Conclusions:** Our findings demonstrate that intratumor heterogeneity represents a challenge for the establishment of a robust HCC classification and may contribute to treatment failure and drug resistance in many cases of HCC.

Introduction

Hepatocellular carcinoma (HCC) generally arises in the context of chronic liver diseases, including chronic viral hepatitis, alcohol-induced liver injury, or other metabolic, dietary or toxic factors such as fatty liver disease or aflatoxin ingestion [1] and ranks number three among the leading causes of cancer mortality worldwide [2]. It is worthy of note that dietary induced liver cancer is one the fastest growing cancer in the United States of America [3]. For a pathologic stratification, tumor stage and grade are the only valid prognostic factors to date. Attempts to classify HCC by immunohistochemical markers or molecular genetic characteristics added fundamental knowledge to our understanding of hepatocarcinogenesis, but so far have hardly been applied in routine surgical pathology and postoperative management [4, 5]. This stands in contrast to the widely accepted classification of hepatocellular adenoma based on morphology, immunohistochemistry and genetics that has been included in the latest edition of the WHO classification [6, 7], and has implications for patient management.

It is well-known that HCC frequently display heterogeneous growth patterns and/or cytological features within one and the same tumor. This might either reflect plasticity of phenotypes or intratumor genetic heterogeneity. Both have been described in several solid tumor entities, including skin, breast, and kidney cancer [8-12]. In small HCC, intratumor heterogeneity with respect to histological differentiation grade and proliferative activity was reported to occur in up to 64% of HCC measuring 3-5 cm in diameter and in 25-47% of HCC smaller than 2 cm [13, 14]. Nonetheless, especially in larger HCC the true extent of intratumor heterogeneity with respect to morphological, immunohistochemical and molecular features has not been systematically assessed. The aim of this study was to systematically investigate intratumor heterogeneity in HCC by a comprehensive analysis of tumor area-specific morphology, correlated with clinically relevant immunohistochemical markers [15-21]. CK7 is a marker of biliary as well as progenitor cell differentiation. CK7/19, in conjunction with *TP53* mutations, has been described as a marker of putative HCC progenitor cells [15] and its expression has been correlated to early tumor recurrence [22]. Likewise, CD44,

EpCAM and AFP have been described to be expressed in hepatic progenitor cells and/or hepatocellular carcinoma [18-21]. In addition, AFP is a serum marker for HCC [23]. The enzyme glutamine synthetase (GS), a marker of pericentral nonneoplastic hepatocytes, is an indicator of Wnt signaling, and together with nuclear accumulation of β -catenin a surrogate marker for *CTNNB1* gene mutations [17, 24]. Analyses were supplemented by multiregional amplicon sequencing of the two genes most frequently mutated in HCC, *TP53* and *CTNNB1* (β -catenin) [5, 23, 25, 26].

Material and Methods

Patients and tissues

23 patients with an initial diagnosis of a primary hepatocellular carcinoma (HCC) receiving surgical treatment between 2003 and 2009 at the University Hospital Zurich were included in this study. Excluded were cases with any kind of pretreatment (e.g. chemotherapy, TACE) and cases with substantial tumor necrosis (>20%). Necrotic tumor areas, ranging between 3-20%, were not included in the analyses. Tumor and adjacent normal liver tissues were formalin-fixed, paraffin embedded (FFPE) and cut into 2-3 μ m sections. Histologic slides were stained with hematoxylin & eosin and scanned with a Hamamatsu NDPI Nano Zoomer (Hamamatsu, Japan). Tumor stage was determined according to the 2009 TNM classification (7th Edition). Tumor grade was assessed according to Edmondson and Steiner [27]. This study was approved by the local ethics committee (StV 26-2005 and KEK-ZH-Nr. 2013-0382).

Morphology and definition of tumor areas

21 of the 23 HCC were single tumors, and only a single lesion was analyzed in two multifocal HCC. Thus, all tissues analyzed of an individual case originated from the same lesion. To distinguish different areas within the same tumor, scanned images were annotated with the Hamamatsu viewer software (NDPI, version 2.2.6). A tumor size range between 0.5 cm and

18 cm was arbitrarily divided into large ($>4\text{cm}$, $n=14$) and smaller HCC ($\leq 4\text{cm}$, $n=9$). The following criteria were used to define specific intratumor areas on HE slides: intratumor fibrotic septa, "nodule-in-nodule" growth and different clearly demarcated architectural growth patterns. In HCC $>4\text{cm}$ up to three tumor blocks were analyzed. At least one area was defined per block, resulting in a minimum of 3 analyzed intratumor regions per large HCC. In smaller HCC ($\leq 4\text{cm}$), 3 areas per tumor from one tumor block were analyzed. Tumor satellite nodules were excluded from the analysis.

The architectural growth patterns of individual tumor areas (solid, pseudoglandular and trabecular) were defined according to the WHO classification 2009 [1]. Additionally, the presence of typical cytological features such as clear cell aspect, fatty change and pleomorphic cells was analyzed. The morphology was designated as heterogeneous if different architectural pattern and/or cytologic features were detectable within the same tumor.

Microdissection of the defined tumor areas was performed by punching two 0.6 mm cores from FFPE tissue blocks with a tissue micro-arrayer (Estigen, MTA1). To minimize potential wild type contamination, dissection marks of every tumor block were evaluated after the dissection procedure by cutting 30 consecutive sections, followed by additionally staining the last slide of every series.

Immunohistochemistry

All slides were stained with antibodies against cytokeratin 7 (CK7), cytokeratin 19 (CK19), CD34, CD44, epithelial cell adhesion molecule (EpCAM), α -fetoprotein (AFP), β -catenin and glutamine synthetase (GS), a downstream target of β -catenin [28, 29] using the following antibodies: CK7: Dako M7018 Cl. Ov-TI 12/30, dilution 1/100; CK 19: Abcam ab 9221, dilution 1:200; CD34: Ventana QBEnd/10 (pre-diluted); CD44: Becton Dickinson G44-26, dilution 1/100; EpCAM: Dako Ber-EP4, dilution 1/40; AFP: Ventana polyclonal, dilution 1/40; glutamine synthetase: Abcam ab 16802 polyclonal, dilution 1:800 and Biocare Medical Cl. 6, dilution 1/500; β -catenin: Transduction lab Inc. 610154 Cl. 14, dilution 1/50. Glutamine synthetase and CK7 were prepared as single and double stainings (opti view, Ventana) with

individual pretreatments (GS: CC1 mild, CK7: Protease 4'). All other stainings (Ventana GX and Ventana Bench Mark Ultra) were performed as single stainings: CD34 (Ventana ultra view, CC1 mild), CD44 (Ventana ultra view, CC1 8'), AFP (Ventana opti view, CC1 mild), CK 19 (Ventana ultra view, P1 4'), and β -catenin (Ventana ultra view, CC1 mild).

A two point score was applied for glutamine synthetase (negative vs. positive) and for β -catenin (nuclear vs. non-nuclear staining). For CK7, CK19, CD34, CD44 and AFP staining, the percentage of immunoreactive cells with respect to each tumor area was semiquantitatively evaluated and grouped according to previously described scoring systems [15] > 50 % positive cells, 5 – 50 % positive cells, < 5 % positive cells (also referred to as scattered cells) or negative. Intratumor expression was considered heterogeneous if expression intensities ranged from “negative” to “positive” (for glutamine synthetase), from “nuclear” to “non-nuclear” (for β -catenin) or from “negative” to \geq 5% positive cells (CK7, CK19, AFP, CD34, CD44). All staining intensities were compared to peritumoral liver tissue. Morphology and immunohistochemistry results were evaluated by at least two different pathologists (JF and LF or AW).

DNA extraction and Sanger sequencing

DNA was extracted from the microdissected tumor areas using a DNA extraction and purification kit adapted for FFPE samples (NucleoSpin, FFPE DNA, Machery-Nagel and GFX PCR purification, GE healthcare). For amplification of exon 5-8 of the *TP53* gene oligonucleotide primer pairs were used as described [30]. PCR was performed in a total volume of 50 μ l with 100-150 ng purified tumor DNA, 0.2 mM dNTPs, 2.5 mM $MgCl_2$, 400nM primer mix (forward and reverse), and 1 unit Taq-polymerase (Amplitaq Gold, Applied Biosystems). The S1000 Bio-Rad thermocycler (Bio-Rad laboratories, Cressier, Switzerland) was used for amplification (95°C initial denaturation, 5min; 40 cycles of 58°C annealing for *TP53* (45s) / 57 °C for *CTNNB1* (1 min); elongation at 72°C (45s for *TP53* / 1 min for *CTNNB1*); final elongation step at 72°C for 7 min (*TP53*) / 10 min (*CTNNB1*)). A BigDye Terminator kit version 3.1 was used for sequencing reactions. For sequencing *CTNNB1* we used an inner forward primer (5'-TAAAGTAACATTTCCAATC-3'). Capillary electrophoresis

was performed on an ABI 3130 xl DNA analyzer (Applied Biosystems). Sequences were analyzed using Bioedit software and BLAST <http://blast.ncbi.nlm.nih.gov/Blast.cgi>. Mutations were identified by comparison with reference sequences (*CTNNB1*- NM_1904.1, *TP53*- NM_001126112.2) and described according international conventions [31].

HCC that showed intratumor heterogeneity on the molecular level by Sanger sequencing were additionally re-sequenced by deep sequencing on a 454 Junior Sequencer platform (Roche, Basel, Switzerland).

DNA quantification and amplicon library preparation for deep sequencing

Amplicon library preparation started with the target specific amplification using bidirectional fusion primers as described earlier [30]. *CTNNB1* fusion primers were designed using NetPrimer software (www.premierbiosoft.com; see supplementary table 1). Primers carried adaptor sequences and individual multiplex identifiers (MIDs). A single amplification step was applied for *TP53* exon 5-8 in 50 µl reactions containing 50 ng of tumor DNA from FFPE samples, 0.2 mM dNTPs, 0.5 mM MgCl₂, 200 nM fusion primer and 1 unit iProof Polymerase (Bio-Rad, Cressier, Switzerland). After 2 min initial denaturation at 98°C, each amplification cycle was performed as follows: 15s denaturation at 98°C, 30s annealing with 58°C annealing temperature for exon 5 and 6, 56°C for exon 7, and 62°C for exon 8 of *TP53* and 30s elongation at 72°C. Final elongation was performed at 72°C for 5 min after 40 cycles.

A two-step amplification protocol for exon 3 of *CTNNB1* was used. The first step included a pre-amplification with the outer forward primer that was used in Sanger sequencing (forward1) and reverse primer (supplementary table 1). Reactions were carried out in 20 µl volume containing 25 ng of DNA, 0.2 mM dNTPs, 0.5 mM MgCl₂, 200 nM fusion primer, 0.5 units iProof polymerase (Bio-Rad laboratories Switzerland, Cressier) and eighteen amplification cycles at 53°C annealing temperature. For the second amplification step, the PCR products of β-catenin were diluted 1:50 and admixed to 0.2 mM dNTPs, 0.5 mM MgCl₂, 400 nM of fusion primer mix (forward 2 and reverse in supplementary table 1), 1 unit iProof polymerase (Bio-Rad Switzerland). Amplification program: 2 min initial denaturation at 98°C; 35 cycles of 15s denaturation at 98°C, 30s annealing at 56°C, 30s elongation at 72°C; final

elongation at 72°C for 5 min. Amplicon purification and quantification were performed with an Augencourt Ampure Kit (Beckmann Coulter, Beverly, USA) and a QuantIT PicoGreen dsDNA assay kit (Invitrogen, Life Technologies, Lucerne, Switzerland), respectively. The diluted library with pooled equimolar amounts of 1×10^5 molecules/ μ l served as input for emPCR (Lib-A by Roche, Basel, Switzerland) reactions (30ul of 1×10^5 molecules for A-beads and 30ul of 1×10^5 molecules for B-beads resulting in a molecule per bead ratio of 0.6:1).

Deep sequencing workflow and analysis

For the target regions exon 3 of *CTNNB1* and exons 5-8 of *TP53*, deep sequencing was performed on a 454 Junior Sequencer (Roche, Basel, Switzerland). Demultiplexing, gene mapping and variant calling (reference genome GRch37/hg19) were performed with Amplicon Variant Analyser software (AVA) version 2.7 from Roche with default settings. We included variants that were present in forward and reverse sequences and with at least 50 reads for further analysis [30]. For quality control (sensitivity and specificity) we amplified the target regions from independent samples of FFPE extracted tumor DNA and sequenced each in an individual run. This resulted in 8 independently amplified and sequenced replicates. In this re-sequenced control we detected the *TP53* variant p.E258V in six of seven runs (sensitivity). The background error rate or “noise” (specificity) was calculated from the frequencies of unexpected single nucleotide changes, insertions or deletions with very low frequencies and/or strand bias that were detected in only one of seven replicate analyses (Supplementary figure 1). One single nucleotide change with a strand bias (fw/rev ratio 2.3) located at a stretch of 4-homopolymers most probably represented a false positive call. As a result the calculated error rate of our control was 1.3% over all amplicons. Variants that could only be detected in deep sequencing and not in Sanger sequencing, i.e. < 10% frequency, were carefully analyzed for strand biases and coverage: if the minimum coverage of an identified variant was <1000 or had a strand bias > 1.5, these areas were re-sequenced. To determine single nucleotide variants and the pathogenicity of mutations, every variant was annotated with an algorithm using free access databases. Annotations were taken from: ENSEMBL (www.ensembl.org), mutations assessor (www.mutationassessor.org), Polyphen

(www.genetics.bwh.harvard.edu/pph), SIFT (www.sift.jcvi.org) and CHASM (www.chasmsoftware.org).

Statistical analysis was conducted by SPSS 20. Analysis of associations between variables was calculated with the Fisher's exact test. Statistical analysis performed on the level of all defined tumor areas was regarded as exploratory since these areas were not completely independent due to the fact that several of these belonged to the same tumor. Survival analysis was performed by Kaplan-Meier analysis and log rank tests. A p-value <.05 was considered as significant. Hierarchical cluster analysis used the squared Euclidean distance as distance measure.

Results

Overall frequency of intratumor heterogeneity in hepatocellular carcinoma

In 23 HCC, a total of 120 tumor areas were demarcated. Per tumor, a mean of five areas (5.3 SD +/- 2.6, range 3-10) was analyzed. The size of the tumor areas ranged from 3-332 mm² (mean 81 SD +/- 80mm²). Intratumor heterogeneity was found with respect to three different features: morphology, immunohistochemistry and mutational status of *CTNNB1* and *TP53* (figure1). A strict hierarchy of features was observed: If tumors showed intratumor heterogeneity for only one feature this feature was morphology (n=6), heterogeneity for two features comprised morphology and immunohistochemistry (n=9), and a combination of all three features (morphology, immunohistochemistry and mutations) was found in 5 cases. Intratumor heterogeneity with respect to the mutational status was always accompanied by heterogeneity on the morphological and immunohistochemical level. Morphological intratumor heterogeneity disregarding other aspects was seen in 87% of HCC. Most commonly the tumors were of solid growth pattern, followed by pseudoglandular growth and trabecular growth pattern (53%, 24% and 23% respectively, quantification based on tumor areas). Ten HCC displayed one or more cytologic features (clear cell n=5, fatty change n=5, pleomorphic cells n=2, bile plugs n=1) in at least one tumor area. Five HCC displayed different histologic grades in the same tumor. However, there was no significant correlation

between specific morphologic patterns, histologic differentiation grades or cytological features and positivity of certain immunohistochemical markers (supplementary table 2). Three tumors were homogeneous, meaning that there was no variation in morphology or immunohistochemical marker expression within the tumor.

Clinico-pathological findings

The mean age of the patients was 62 years (SD +/- 12.4), and the male/female ratio was 3.8/1. The mean size of the tumors (range 0.5-18cm) was 7.4cm SD +/- 5.4cm. Large HCC (n=14) had a mean tumor size of 10 cm (SD +/- 4) and small HCC (n=9) had a mean tumor size of 2 cm (SD +/- 0.7).

Table 1 shows the tumor-specific findings and associated clinical background. The tumors were sorted by size and stratified according to TNM (2009) with a distribution of 6/14/3 for the tumor stages pT1/T2/T3. Genetic intratumor heterogeneity was more frequently seen in tumors with higher tumor stages (n=4/17 of tumor stage T2 and T3) and larger tumor size of >4cm (n=4/14). Multinodularity of tumors was frequently associated with morphological and combined immunohistochemical intratumor heterogeneity (p=.023), whereas satellite nodules were generally a rare finding (4/23). 60% of HCC with molecular heterogeneity, 56% of HCC with immunohistochemical heterogeneity and 33% of HCC with morphological heterogeneity showed vascular invasion. The median disease free survival was not significantly different between the two groups (26 months in the 5 patients with tumors displaying genetic heterogeneity, compared to 27 months in other patients). Of four tested pathological variables (intratumor heterogeneity, multinodularity, satellite nodules, vascular invasion) only vascular invasion showed significant impact on patient survival (log rank test: p=.04, supplementary figure 2).

Twenty HCC patients were known to have a chronic liver disease. Eleven patients suffered from chronic hepatitis B or C. Three patients had HCC of unknown etiology. In a total of 5 cases in which tumors displayed all features of intratumor heterogeneity (morphology, immunohistochemistry and molecular characteristics) there was no predominance of a particular chronic liver disease. Worthy of note is that 2 of 3 patients with HCC of unknown etiology had homogeneous tumors.

Intratumor heterogeneity of immune phenotypes

Table 2 provides a heatmap of intratumor heterogeneity of immune phenotypes. Eleven tumors were glutamine synthetase positive and/or showed β -catenin nuclear positivity in at least one tumor area. The association between these two markers was in line with published data [24, 29] and found to be statistically significant ($p=.006$). Consistent glutamine synthetase positivity in all areas of the same tumor was found in only 2 cases, whereas heterogeneous immunoreactivity of glutamine synthetase was seen in 80% of the tumors ($n=8/10$). Of 15 CK7 positive tumors, 73% exhibited intratumoral heterogeneous CK7 expression ($n=11/15$). CK7 positivity in all tumor areas of the same tumor was found in 4 HCC. In tumors with intratumoral heterogeneous CK7 expression, a spectrum of different staining patterns was observed: exclusive positivity in glandular structures, widely scattered single cell staining, or marked foci within single tumor areas (supplementary figure 3). CD44 expression was found in ten tumors, with 4 showing intratumoral heterogeneous expression. 57% of AFP positive tumors showed intratumoral heterogeneous expression ($n=4/7$). Immunohistochemical AFP expression (heterogeneous and homogeneous) was significantly associated with increased serum AFP (pre-surgical measurements) $>10 \mu\text{g/l}$ ($p=.015$). One HCC exhibited foci of immunoreactivity for EpCAM in single tumor areas (patient 3). Strong positivity over all tumor areas was seen in a young patient with a hepatitis B-related HCC (patient 14).

In the analysis of area-specific morphology with respect to immunohistochemistry, no significant associations between morphological growth pattern and cytologic features were detected (supplementary table 2). Remarkably, 71% of areas with clear cell aspect and 48% of pseudoglandular areas showed CK7 positivity.

CK19 positivity was only present in entrapped bile ducts. Similarly, CD34 expression was not found in tumor cells, but only in microvessel structures (not shown). Figure 2 illustrates overview and high power of intratumor heterogeneity of all three features (patient 13). Tumor areas were defined and schematically illustrated by the H&E slide overview. Microscopy images showed predominantly solid growth pattern with partial glutamine synthetase or CK7 positivity. Multiregional sequencing revealed three different *CTNNB1* mutations: a private

S37 and two shared mutations (T41 and 15bp deletion at c.352-c.367), while a single nucleotide polymorphism in exon 6 of TP53 (rs 1800372) was detected in all tumor areas.

Intratumor diversity of *CTNNB1* and *TP53* mutational status in HCC

Of 23 HCC, six were *CTNNB1* mutated and two were *TP53* mutated. *CTNNB1* mutations affected the GSK-3 β phosphorylation sites, as described [25], and were significantly associated with immunohistochemical positivity for glutamine synthetase ($p=.002$) as well as nuclear accumulation of β -catenin ($p=.009$).

A total of 120 tumor areas in 23 HCC were sequenced targeting *CTNNB1* and *TP53*. The distribution of wild type, *CTNNB1* and/or *TP53* mutated tumor areas is shown in table 1 and illustrated for intratumoral heterogeneous cases in figure 2, figure 3 and supplementary figure 4 A. For eight HCC cases, all tumor areas were validated using deep sequencing to detect mutations with low frequencies and to account for the possibility that wild-type contamination might have led to false-negative results using the Sanger sequencing method. Targeted deep sequencing was performed in 8 individual runs. A total load of ~500,000 enriched beads per run resulted in an average of 79867 high quality reads with a mean coverage of 1442 reads per amplicon. Two additional low frequency *CTNNB1* mutations were discovered by deep sequencing. For example, Sanger sequencing detected a *CTNNB1* mutation (I35S) in 5/6 tumor areas in patient 1, whereas 6/6 areas were mutated at the same location in deep sequencing (supplementary figure 4 B). Another additional low frequency *CTNNB1* mutation (S37P) was detected in patient 2 (figure 3 C). Conversely, two *CTNNB1* mutations that were detected in tumor areas of patient 2 (S45P, figure 3 C) and of patient 19 (E54E, not shown) could not be validated in deep sequencing (coverage: 2297 and 2111 reads respectively). Remarkably, two HCC with heterogeneous intratumor morphology and immunohistochemistry of three markers (CK7, glutamine synthetase and β -catenin nuclear accumulation) exhibited different *CTNNB1* mutations in different tumor areas (figure 2 and 3 C). Moreover, one tumor (patient 2) carried three different *CTNNB1* mutations in one single area (figure 3 C), displaying a rare L31P, a S33A and a silent mutation P44P (P44P not shown). Analysis of single reads of deep sequencing results revealed that not all nucleotide exchanges were located on the same read (data not shown). Two HCC carried *TP53*

mutations, one in exon 5 and one in exon 7. Intratumor heterogeneity with wild type and *TP53* mutated tumor areas was seen in one patient with a R175H mutation (patient 6, figure 3 E). Another *TP53* mutation (E258G) was found in all tumor areas in patient 4. Analysis for single nucleotide polymorphisms of the targeted genes (exon 3 *CTNNB1*, exon 5-8 *TP53*) were also taken into account for determining molecular intratumor heterogeneity. Only a single nucleotide polymorphism (rs 1800372) was uniformly detected in the HCC of patient 13 along with intratumoral heterogeneous *CTNNB1* mutations (figure 2 D). Multiregional sequencing results were finally displayed as hierarchical cluster analysis (dendrograms of figure 2 D, 3 B, D, F) showing clusters of mutated among wild type tumor areas.

Area-based analysis of mutational status, the expression of immunohistochemical markers and morphology revealed a positive association between *CTNNB1* mutations, nuclear β -catenin [24] and glutamine synthetase positivity [29]. *CTNNB1* mutations and AFP positivity were inversely associated as has been observed before [32]. Furthermore, a pseudoglandular growth pattern was frequently seen in *CTNNB1* mutated tumor areas (45%). CD44 positivity was present in 70% of *TP53* mutated areas [33]. The association between *TP53* mutation and β -catenin immunohistochemistry found in our cohort was due to a single *TP53* mutated HCC (patient 4) with nuclear β -catenin staining in all tumor areas (table 3).

Discussion

In this study we systematically characterized intratumor heterogeneity in hepatocellular carcinoma (HCC) on the level of morphology, immune phenotype, or mutational status of *CTNNB1* and *TP53*, respectively. With this approach, we found tumor heterogeneity of at least one feature in the majority of HCC (20/23; 87%). Although based on a relatively small number of cases, our findings have implications for HCC biology, HCC classification and HCC targeted therapy in the era of personalized medicine.

Morphological intratumor heterogeneity in HCC has been reported before by Kenmochi et al. [13], who found two or more histological differentiation grades in more than half of the cases they had studied. An and coworkers [14] also analyzed heterogeneity with respect to the histological grade and described different tumor grades in 11 of 41 surgically resected small HCC (< 3 cm in diameter). After studying tumor heterogeneity on three different levels, we now confirm and further define this phenomenon, having detected heterogeneity in different combinations revealing a strict hierarchy: 1) either only on the level of morphology, 2) or morphological heterogeneity combined with immunohistochemical heterogeneity, 3) or a three feature intratumor heterogeneity with respect to morphology, immunohistochemistry and the mutational status of *TP53* and *CTNNB1*. Morphological and immunophenotypical heterogeneity within a tumor might either reflect variable genetic aberrations or tumor cell plasticity without underlying genetic differences. Our data suggest that both apply to HCC. Notably, about 50% of HCC reveal heterogeneous expression of two key immunohistochemical markers in liver pathology, i.e. CK7 and glutamine synthetase (GS), respectively, which also are used for HCC classification and prognostication [15]. Not unexpectedly, we observed that the frequency of morphological intratumor heterogeneity was associated with larger tumor size and higher tumor stage, although it did not reach statistical significance, most likely due to a small sample size.

Studying *TP53* and *CTNNB1*, we found a heterogeneous intratumor mutational status in 22% of HCC. Different types of *CTNNB1* mutations in one tumor sample were also reported before by Van Nieuw et al. [34] and Huang et al. [35]. Park et al. analyzed HCC as well as precursor lesions for the presence of *CTNNB1* mutations, and found no *CTNNB1* mutations in precursor lesions of HCC [36]. These findings show that *CTNNB1* mutations, generally considered as driver mutations in HCC, are not uniformly present in all tumor regions within the same tumor, and reflect a rather late event in hepatocarcinogenesis. *TP53* and *CTNNB1* are both used as molecular classifiers for hepatocellular carcinoma [26, 37]. For instance, the transcriptome classification proposed by Boyault et al. depicts 6 subgroups of HCC; two groups are associated with *TP53* and two other groups with *CTNNB1* alterations [37]. The intratumor heterogeneity we found on the molecular and morphological level indicates a high degree of genetic instability in HCC. This stands in contrast to hepatocellular adenoma, for

which a solid body of literature exists without evidence for relevant histological heterogeneity [38, 39]. Furthermore based on the few data available on genetic heterogeneity in hepatocellular adenoma (HCA) when progression to HCC was studied [40], it can be assumed, that adenoma are more homogeneous. The classification of HCA based on the clinical setting, morphology and genetics is well accepted [6], and has an impact on the clinical management of HCA patients. For HCC, classification proposals based on genetic changes [26], or gene expression patterns [41, 42], have not proven robust enough so far to be integrated into clinical practice. According to our data, intratumor heterogeneity obviously is an obstacle to the establishment of a comprehensive classification of HCC comparable to the HCA classification [6, 7]. Distinct parts of one and the same tumor differ with respect to biomarker expression and mutational status, which illustrates the co-existence of different tumor-cell populations in the same tumor. Presumably, the rate of genetic diversity would be even higher if the genetic analysis of individual tumor areas were expanded to analyze more genes.

Molecular analysis, based on testing a small piece of tumor, might underestimate the complexity of tumor genomics. According to our data which are based on analysis of multiple tumor regions, single tumor biopsies might be an insufficient approach to characterize individual HCC. It is conceivable that a significant proportion of HCC already harbor the same genetic complexity and molecular heterogeneity within one and the same tumor that is characteristic of HCC as a tumor entity [1, 43]. This obviously impedes the development of a comprehensive and clinically meaningful HCC classification.

The level of intratumor heterogeneity we have demonstrated may result in evasion of therapy when targeting single molecules of hepatocarcinogenesis. In particular, the wnt/ β -catenin pathway is discussed as a potential therapeutic target in HCC [44]. Since the efficacy of a molecular therapy is determined by the mutational status of the target, e.g. EGFR in colorectal and lung cancer treatment, or c-KIT in the case of GIST, an HCC harboring tumor subpopulations with variable *CTNNB1* mutational status (notably prior to therapy) is a major challenge. Currently, treatment with the multi-targeted tyrosine kinase inhibitor sorafenib is the only proposed molecular targeted therapy for HCC, although only a modest survival benefit was demonstrated in a multicenter European HCC trial [45], and even markedly lower

benefit in a trial with Asian HCC patients [46]. The intratumoral molecular diversity we have shown for the *TP53* and *CTNNB* mutational status in a significant proportion of HCC suggests that the development of a molecular targeted therapy for HCC might be more challenging than for tumor entities with more uniform targetable genetic changes.

In summary, in a comprehensive analysis on the level of morphology, immunohistochemistry, and mutational status of *TP53* and *CTNNB* genes, we show that intratumor heterogeneity is a frequent finding in HCC. This finding might be the reason for some of the challenges in developing a robust classification of HCC as well as a molecular targeted therapy for this tumor entity.

Acknowledgements

The authors would like to thank Marion Bawohl, Anette Bohnert and Renaud Maire for their excellent technical assistance.

Figure legends

Figure 1: Frequency of intratumor heterogeneity with respect to different criteria (morphology, immunohistochemistry and mutational status of *CTNNB1* and *TP53*) in 23 HCC.

Figure 2: HCC in patient 13 (60y, male, history of alcohol and diabetes II). **A:** Slide overview (H&E staining) and photomicrographs of defined tumor areas, scale bar: 5 mm. **B:** Microscopy images (40x) of tumor areas consecutively revealed by H&E staining, CK7, glutamine synthetase (GS) and β -catenin immunohistochemistry, scale bar: 40 μ m. **C:** Morphological, immunohistochemical and molecular characterization of numbered tumor areas; (+) Morphological pattern present or immunohistochemistry positive (glutamine synthetase: positive, CK7: $\geq 5\%$, β -catenin: nuclear staining); empty spaces: morphological pattern absent or negative immunoreaction; sc- scattered cells, ic- immunohistochemistry, Sanger seq- Sanger sequencing, deep seq- deep sequencing **Mutations:** chromatograms from Sanger sequencing and global alignment graph of 454 analysis output (AVA software), purple square: codon number of *CTNNB1* or *TP53* gene and amino-acid exchange thereof compared to reference sequences NM 1904.1 (*CTNNB1*) and NM 001126112.2 (*TP53*). bp del base pair deletion, wt- mutational analysis wild type. **D:** Dendrogram of clustered tumor

areas (hierarchical clustering) according to private mutations in single tumor areas (S37), shared mutations (T41, 15 bp deletion) and ubiquitous single nucleotide polymorphism in exon 6 of *TP53* (rs1800372). Distance measure: squared Euclidean distance.

Figure 3 A, C, E: Morphological, immunohistochemical and molecular characterization of numbered tumor areas in 3 individual patients. (+) Morphological pattern present or immunohistochemistry positive (glutamine synthetase: positive, CK7: $\geq 5\%$, β -catenin: nuclear staining); empty space: morphological pattern absent or negative immunoreaction. ic- immunohistochemistry, sc- scattered cells, Sanger seq- Sanger sequencing, deep seq- deep sequencing. **Mutations:** depicted by chromatograms from Sanger sequencing and global alignment graph of 454 analysis output (AVA software), purple square: codon number of *CTNNB1* or *TP53* gene and amino-acid exchange thereof compared to reference sequences NM 1904.1 (*CTNNB1*) and NM 001126112.2 (*TP53*). wt- mutational analysis wild type. **B, D, F:** Corresponding dendrograms illustrating hierarchical cluster analysis of tumor areas. Distance measure: squared Euclidean distance.

Reference List

- [1] Theise ND, Curado MP, Franceschi S, Hytioglou P, Kudo M, Park YN, et al. Hepatocellular carcinoma. WHO classification of tumors of the digestive system, 4th edition edn. WHO classification of tumors of the digestive system, 4th edition, World Health Organization, Geneva; 2010. p. 205-16.
- [2] Parkin DM, Bray F, Ferlay J, Pisani P. Global cancer statistics, 2002. *CA Cancer J Clin* 2005;55:74-108.
- [3] Michelotti GA, Machado MV, Diehl AM. NAFLD, NASH and liver cancer. *Nat Rev Gastroenterol Hepatol* 2013;10:656-65.
- [4] Nault JC, Zucman-Rossi J. Genetics of hepatobiliary carcinogenesis. *Semin Liver Dis* 2011;31:173-87.
- [5] Nault JC, Zucman-Rossi J. Genetics of hepatocellular carcinoma: The next generation. *J Hepatol* 2013.
- [6] Zucman-Rossi J, Jeannot E, Nhieu JT, Scoazec JY, Guettier C, Rebouissou S, et al. Genotype-phenotype correlation in hepatocellular adenoma: new classification and relationship with HCC. *Hepatology* 2006;43:515-24.
- [7] Bioulac-Sage P, Balabaud C, Wanless I. Focal nodular hyperplasia and hepatocellular carcinoma. WHO classification of tumors of the digestive system, 4th edition edn. WHO classification of tumors of the digestive system, 4th edition, World Health Organization, Geneva; 2010. p. 198-204.
- [8] Gerlinger M, Rowan AJ, Horswell S, Larkin J, Endesfelder D, Gronroos E, et al. Intratumor heterogeneity and branched evolution revealed by multiregion sequencing. *N Engl J Med* 2012;366:883-92.
- [9] Holzel M, Bovier A, Tuting T. Plasticity of tumour and immune cells: a source of heterogeneity and a cause for therapy resistance? *Nat Rev Cancer* 2013;13:365-76.
- [10] Berman HK, Gauthier ML, Tlsty TD. Premalignant breast neoplasia: a paradigm of interlesional and intralesional molecular heterogeneity and its biological and clinical ramifications. *Cancer Prev Res (Phila)* 2010;3:579-87.
- [11] Raychaudhuri M, Schuster T, Buchner T, Malinowsky K, Bronger H, Schwarz-Boeger U, et al. Intratumoral heterogeneity of microRNA expression in breast cancer. *J Mol Diagn* 2012;14:376-84.
- [12] Almendro V, Marusyk A, Polyak K. Cellular heterogeneity and molecular evolution in cancer. *Annu Rev Pathol* 2013;8:277-302.
- [13] Kenmochi K, Sugihara S, Kojiro M. Relationship of histologic grade of hepatocellular carcinoma (HCC) to tumor size, and demonstration of tumor cells of multiple different grades in single small HCC. *Liver* 1987;7:18-26.
- [14] An FQ, Matsuda M, Fujii H, Tang RF, Amemiya H, Dai YM, et al. Tumor heterogeneity in small hepatocellular carcinoma: analysis of tumor cell proliferation, expression and mutation of p53 AND beta-catenin. *Int J Cancer* 2001;93:468-74.
- [15] Durnez A, Verslype C, Nevens F, Fevery J, Aerts R, Pirenne J, et al. The clinicopathological and prognostic relevance of cytokeratin 7 and 19 expression in hepatocellular carcinoma. A possible progenitor cell origin. *Histopathology* 2006;49:138-51.
- [16] Wu PC, Fang JW, Lau VK, Lai CL, Lo CK, Lau JY. Classification of hepatocellular carcinoma according to hepatocellular and biliary differentiation markers. Clinical and biological implications. *Am J Pathol* 1996;149:1167-75.

- [17] Zulehner G, Mikula M, Schneller D, van ZF, Huber H, Sieghart W, et al. Nuclear beta-catenin induces an early liver progenitor phenotype in hepatocellular carcinoma and promotes tumor recurrence. *Am J Pathol* 2010;176:472-81.
- [18] Yamashita T, Forgues M, Wang W, Kim JW, Ye Q, Jia H, et al. EpCAM and alpha-fetoprotein expression defines novel prognostic subtypes of hepatocellular carcinoma. *Cancer Res* 2008;68:1451-61.
- [19] Yamashita T, Ji J, Budhu A, Forgues M, Yang W, Wang HY, et al. EpCAM-positive hepatocellular carcinoma cells are tumor-initiating cells with stem/progenitor cell features. *Gastroenterology* 2009;136:1012-24.
- [20] Schmelzer E, Wauthier E, Reid LM. The phenotypes of pluripotent human hepatic progenitors. *Stem Cells* 2006;24:1852-8.
- [21] Yang XR, Xu Y, Yu B, Zhou J, Qiu SJ, Shi GM, et al. High expression levels of putative hepatic stem/progenitor cell biomarkers related to tumour angiogenesis and poor prognosis of hepatocellular carcinoma. *Gut* 2010;59:953-62.
- [22] Yuan RH, Jeng YM, Hu RH, Lai PL, Lee PH, Cheng CC, et al. Role of p53 and beta-catenin mutations in conjunction with CK19 expression on early tumor recurrence and prognosis of hepatocellular carcinoma. *J Gastrointest Surg* 2011;15:321-9.
- [23] Forner A, Llovet JM, Bruix J. Hepatocellular carcinoma. *Lancet* 2012;379:1245-55.
- [24] Austinat M, Dunsch R, Wittekind C, Tannapfel A, Gebhardt R, Gaunitz F. Correlation between beta-catenin mutations and expression of Wnt-signaling target genes in hepatocellular carcinoma. *Mol Cancer* 2008;7:21.
- [25] de La CA, Romagnolo B, Billuart P, Renard CA, Buendia MA, Soubrane O, et al. Somatic mutations of the beta-catenin gene are frequent in mouse and human hepatocellular carcinomas. *Proc Natl Acad Sci U S A* 1998;95:8847-51.
- [26] Guichard C, Amaddeo G, Imbeaud S, Ladeiro Y, Pelletier L, Maad IB, et al. Integrated analysis of somatic mutations and focal copy-number changes identifies key genes and pathways in hepatocellular carcinoma. *Nat Genet* 2012;44:694-8.
- [27] EDMONDSON HA, STEINER PE. Primary carcinoma of the liver: a study of 100 cases among 48,900 necropsies. *Cancer* 1954;7:462-503.
- [28] Cadoret A, Ovejero C, Terris B, Souil E, Levy L, Lamers WH, et al. New targets of beta-catenin signaling in the liver are involved in the glutamine metabolism. *Oncogene* 2002;21:8293-301.
- [29] Loeppen S, Schneider D, Gaunitz F, Gebhardt R, Kurek R, Buchmann A, et al. Overexpression of glutamine synthetase is associated with beta-catenin-mutations in mouse liver tumors during promotion of hepatocarcinogenesis by phenobarbital. *Cancer Res* 2002;62:5685-8.
- [30] Rechsteiner M, von TA, Ruschoff JH, Fankhauser N, Pestalozzi B, Schraml P, et al. KRAS, BRAF, and TP53 deep sequencing for colorectal carcinoma patient diagnostics. *J Mol Diagn* 2013;15:299-311.
- [31] Ogino S, Gulley ML, den Dunnen JT, Wilson RB. Standard mutation nomenclature in molecular diagnostics: practical and educational challenges. *J Mol Diagn* 2007;9:1-6.
- [32] Gorog D, Regoly-Merei J, Paku S, Kopper L, Nagy P. Alpha-fetoprotein expression is a potential prognostic marker in hepatocellular carcinoma. *World J Gastroenterol* 2005;11:5015-8.
- [33] Endo K, Terada T. Protein expression of CD44 (standard and variant isoforms) in hepatocellular carcinoma: relationships with tumor grade, clinicopathologic parameters, p53 expression, and patient survival. *J Hepatol* 2000;32:78-84.

- [34] Nhieu JT, Renard CA, Wei Y, Cherqui D, Zafrani ES, Buendia MA. Nuclear accumulation of mutated beta-catenin in hepatocellular carcinoma is associated with increased cell proliferation. *Am J Pathol* 1999;155:703-10.
- [35] Huang H, Fujii H, Sankila A, Mahler-Araujo BM, Matsuda M, Cathomas G, et al. Beta-catenin mutations are frequent in human hepatocellular carcinomas associated with hepatitis C virus infection. *Am J Pathol* 1999;155:1795-801.
- [36] Park JY, Park WS, Nam SW, Kim SY, Lee SH, Yoo NJ, et al. Mutations of beta-catenin and AXIN 1 genes are a late event in human hepatocellular carcinogenesis. *Liver Int* 2005;25:70-6.
- [37] Boyault S, Rickman DS, de RA, Balabaud C, Rebouissou S, Jeannot E, et al. Transcriptome classification of HCC is related to gene alterations and to new therapeutic targets. *Hepatology* 2007;45:42-52.
- [38] Bioulac-Sage P, Rebouissou S, Thomas C, Blanc JF, Saric J, Sa CA, et al. Hepatocellular adenoma subtype classification using molecular markers and immunohistochemistry. *Hepatology* 2007;46:740-8.
- [39] Bioulac-Sage P, Cubel G, Balabaud C, Zucman-Rossi J. Revisiting the pathology of resected benign hepatocellular nodules using new immunohistochemical markers. *Semin Liver Dis* 2011;31:91-103.
- [40] Pilati C, Letouze E, Nault JC, Imbeaud S, Boulai A, Calderaro J, et al. Genomic Profiling of Hepatocellular Adenomas Reveals Recurrent FRK-Activating Mutations and the Mechanisms of Malignant Transformation. *Cancer Cell* 2014;25:428-41.
- [41] Lee JS, Chu IS, Heo J, Calvisi DF, Sun Z, Roskams T, et al. Classification and prediction of survival in hepatocellular carcinoma by gene expression profiling. *Hepatology* 2004;40:667-76.
- [42] Lee JS, Heo J, Libbrecht L, Chu IS, Kaposi-Novak P, Calvisi DF, et al. A novel prognostic subtype of human hepatocellular carcinoma derived from hepatic progenitor cells. *Nat Med* 2006;12:410-6.
- [43] Walther Z, Jain D. Molecular pathology of hepatic neoplasms: classification and clinical significance. *Patholog Res Int* 2011;2011:403929.
- [44] Dahmani R, Just PA, Perret C. The Wnt/beta-catenin pathway as a therapeutic target in human hepatocellular carcinoma. *Clin Res Hepatol Gastroenterol* 2011;35:709-13.
- [45] Llovet JM, Ricci S, Mazzaferro V, Hilgard P, Gane E, Blanc JF, et al. Sorafenib in advanced hepatocellular carcinoma. *N Engl J Med* 2008;359:378-90.
- [46] Cheng AL, Guan Z, Chen Z, Tsao CJ, Qin S, Kim JS, et al. Efficacy and safety of sorafenib in patients with advanced hepatocellular carcinoma according to baseline status: subset analyses of the phase III Sorafenib Asia-Pacific trial. *Eur J Cancer* 2012;48:1452-65.

Figure 1

Author Manuscript Published OnlineFirst on September 23, 2014; DOI: 10.1158/1078-0432.CCR-14-0122
Author manuscripts have been peer reviewed and accepted for publication but have not yet been edited.

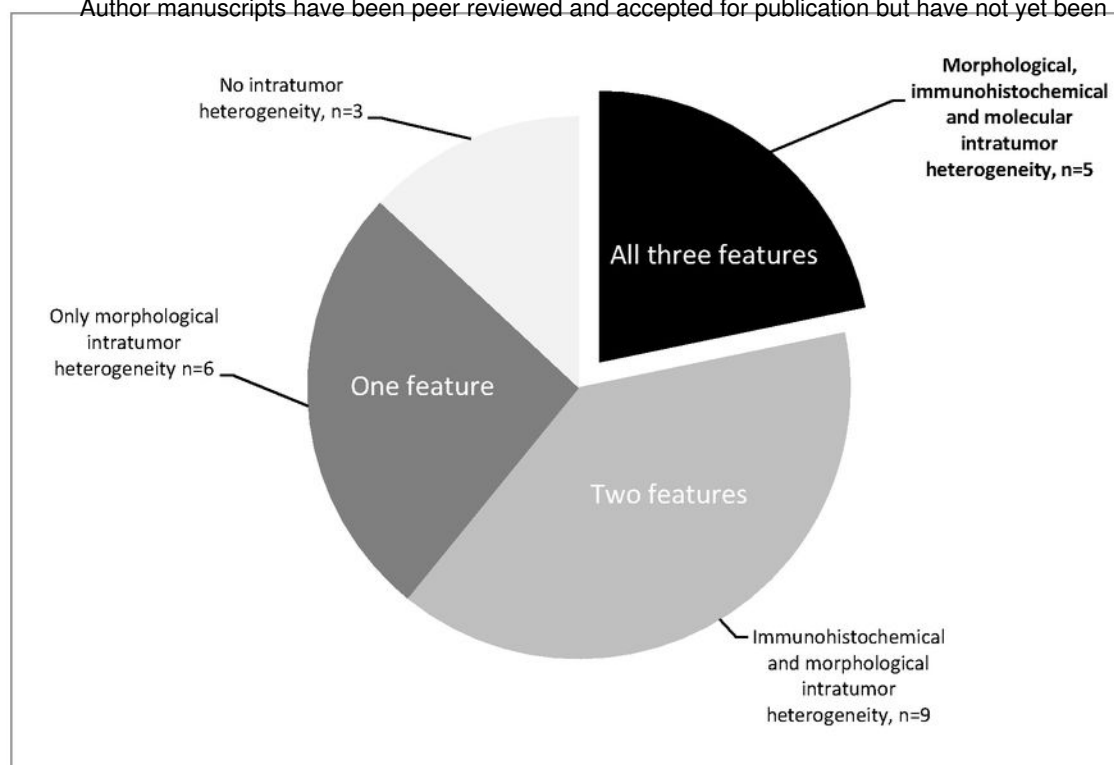
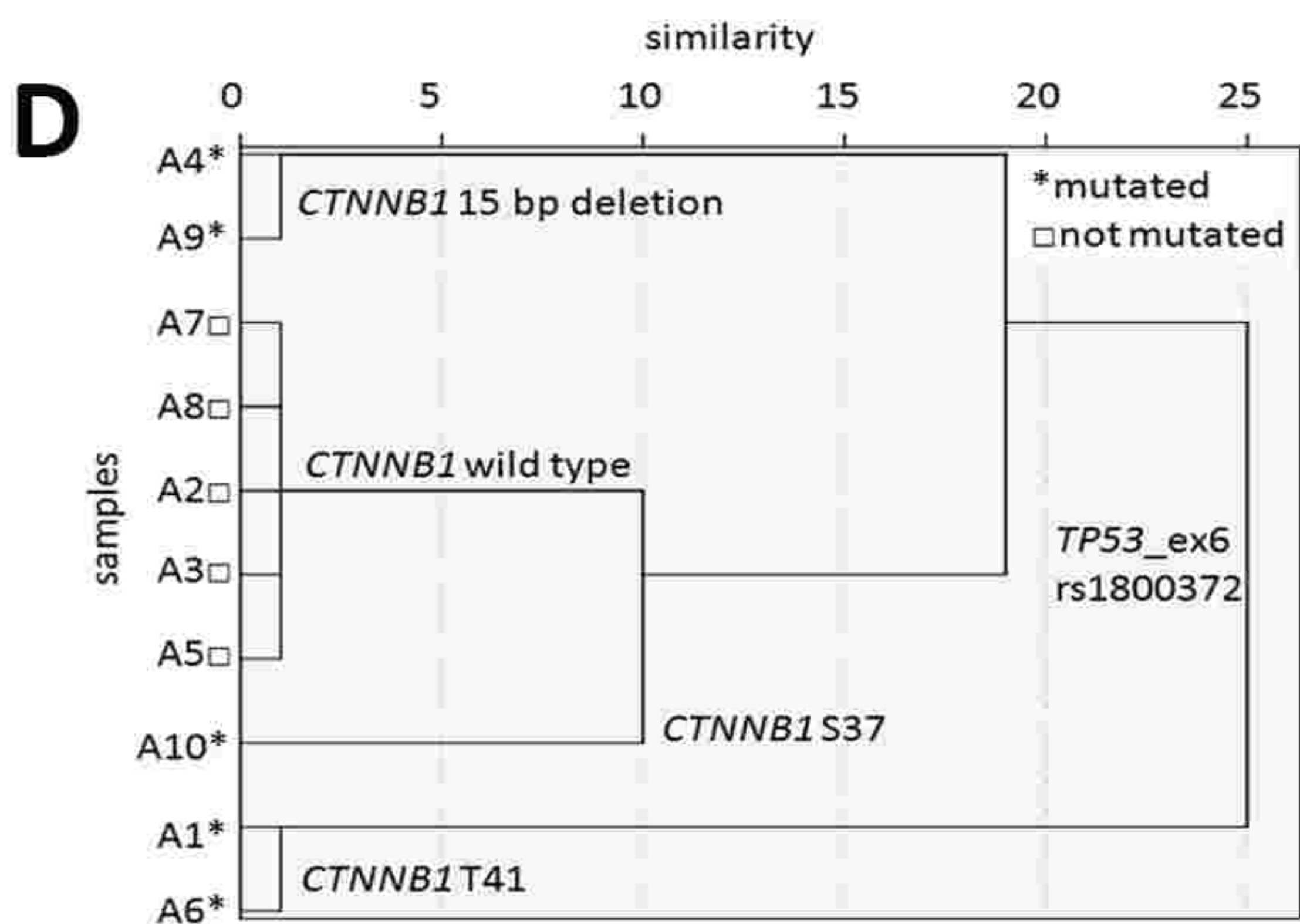
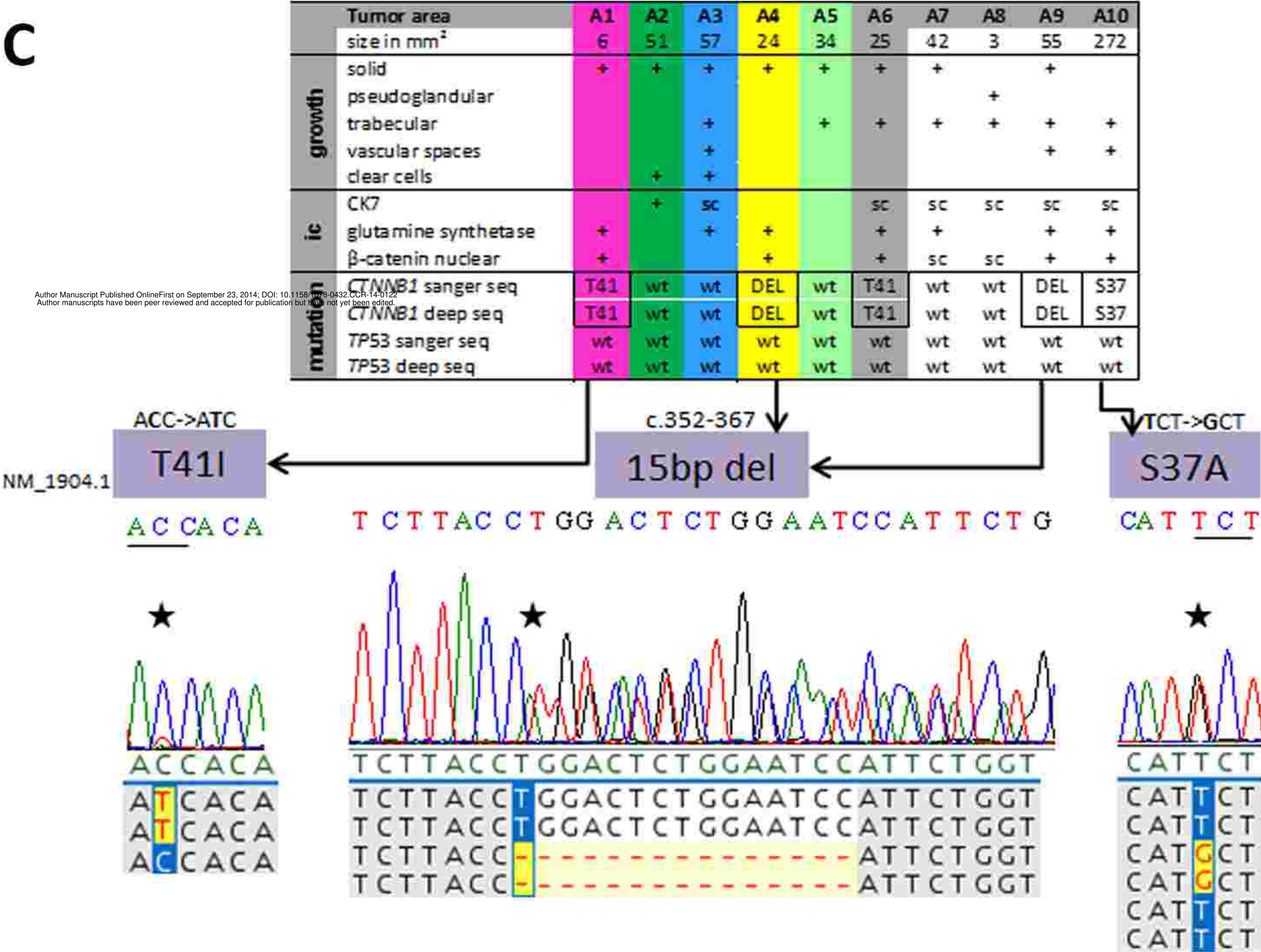
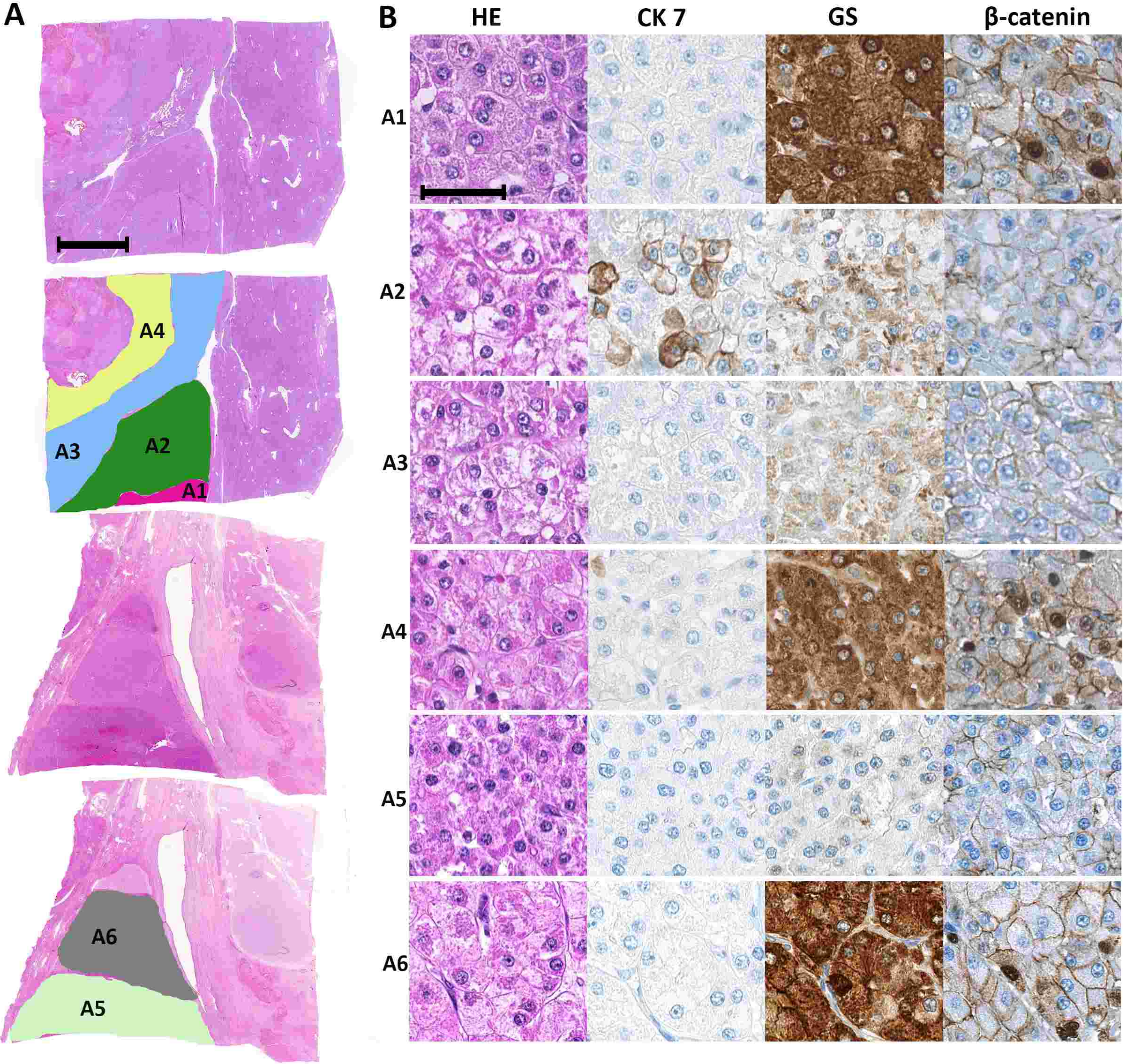


Figure 2



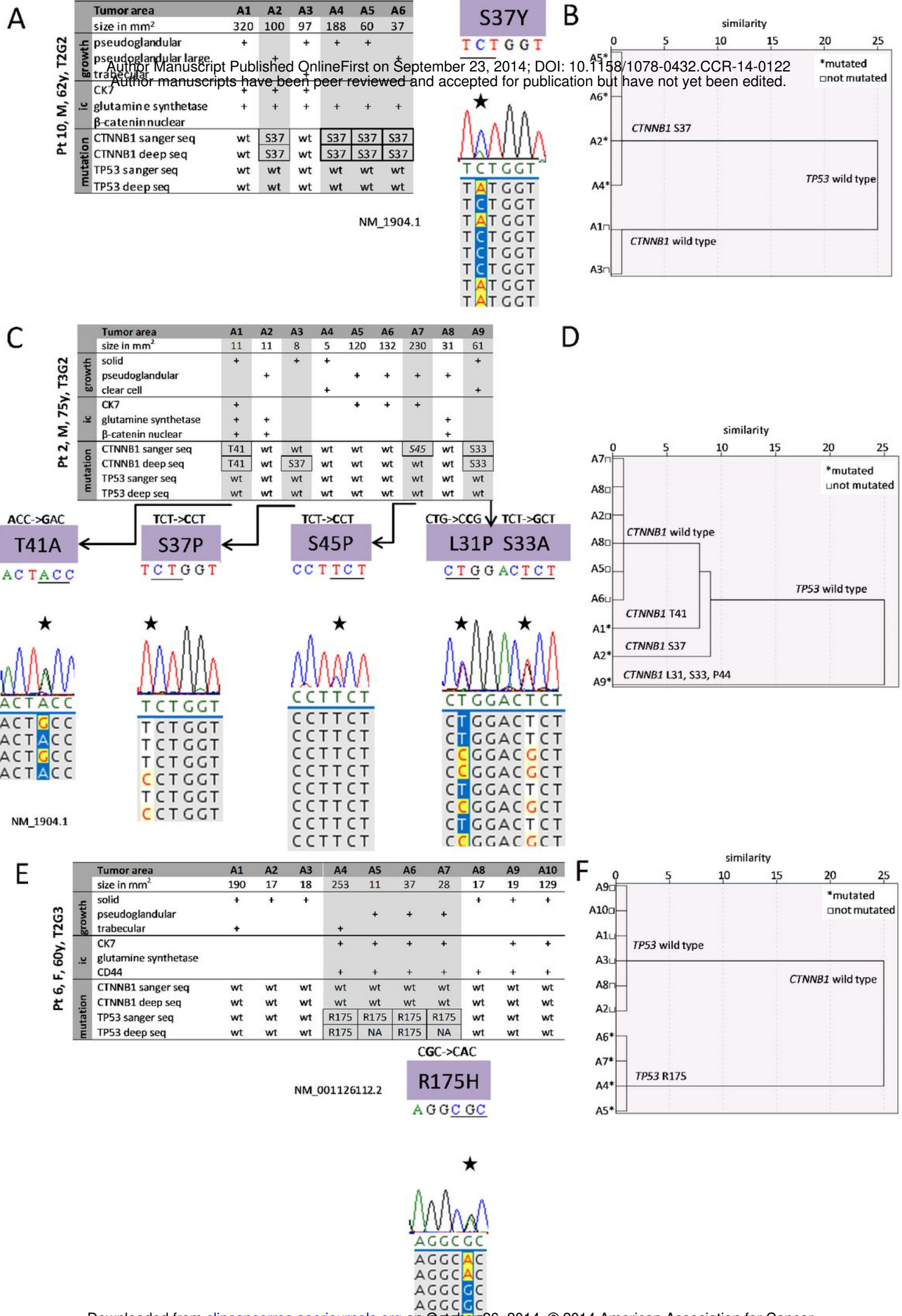


Table 1: Clinical And Pathological Data Of 23 Patients With Hepatocellular Carcinoma (HCC)

Large Hepatocellular Carcinoma 5-18cm (Ø 10cm)

					AFP level Serum (µg/l)	Tumor size (cm)	Tumor stage, vascular invasion	Multinodularity/ Satellites	Features of intra-tumoral heterogeneity	CTNNB1 ^a mutations/analyzed tumor regions	TP53 ^b mutations/analyzed tumor regions
Pt	Sex	Age	Risk factor HCC	Liver histology							
1	M ^e	74	Hepatitis B	Steatosis 40%, Fibrosis periportal	4.4	5,8	pT1G2, ^g V-	+/-	Growth, IC ^c	6/6	0/6
2	M	75	Alcohol	Fibrosis periportal and septal	10	6	pT3G2, V+	+/-	Growth, IC, Mol ^d	3/9	0/9
3	M	57	α1-deficiency	Fibrosis periportal and septal	1389.5	7,5	pT2G2, V+	+/-	Growth, IC	0/6	0/6
4	M	69	Hepatitis B, diabetes II	Fibrosis periportal and septal	NA	8,5	pT1G2, V-	+/-	Growth, IC	0/6	6/6
5	M	63	Unknown etiology	Portal Fibrosis	NA	8,5	pT3aG2, V+	-/+	None	0/3	0/3
6	F ^f	60	Obesity	Steatosis 10-20%	<10	9,2	pT2G3, V+	+/-	Growth, IC, Mol	0/10	4/10
7	M	77	Diabetes II	Fibrosis periportal	126.6	9,5	pT2G2, V+	+/-	Growth, IC	0/8	0/8
8	F	61	Tobacco	Portal Fibrosis	12630	9,8	pT2G2, V+	+/-	Growth	0/7	0/7
9	F	63	Unknown etiology	Portal Fibrosis	NA	10	pT2G3, V+	-/+	None	0/3	0/3
10	M	62	Hemochromatosis	Siderosis, Fibrosis portal	43.2	10,5	pT2G2, V+	+/-	Growth, IC, Mol	4/6	0/6
11	M	80	Tobacco , alcohol	Steatosis 10%	NA	13,5	pT2G3, V+	+/-	Growth, IC	0/7	0/7
12	M	70	Alcohol	Steatosis 20%, Fibrosis portal	85.6	16	pT2G3, V+	+/-	Growth	0/7	0/7
13	M	60	Alcohol, diabetes II	Steatosis	NA	18	pT2G1, V-	+/-	Growth, IC, Mol	5/10	0/10
14	F	23	Hepatitis B	Cirrhosis	16387	18	pT3bG3, V+	+/-	Growth, IC	0/5	0/5

Smaller Hepatocellular Carcinoma 0.5-4cm (Ø 2cm)

					AFP level Serum (µg/l)	Tumor size (cm)	Tumor stage, vascular invasion	Multinodularity/ Satellites	Features of intra-tumoral heterogeneity	CTNNB1 ^a mutations/analyzed tumor regions	TP53 ^b mutations/analyzed tumor regions
Sex	Sex	Age	Risk factor HCC	Liver histology							
15	M	62	Hepatitis B	Incomplett cirrhosis	2.8	0,5	pT2G1, V-	-/-	None	0/3	0/3
16	M	67	Unknown etiology	Cirrhosis	NA	1,5	pT2G2, V-	+/+	Growth	0/3	0/3
17	M	75	Hepatitis C, alcohol	Cirrhosis	NA	1,5	pT2G2, V-	-/-	Growth	0/3	0/3
18	M	45	Hepatitis B, diabetes II	Cirrhosis	NA	2,2	pT1G2, V-	-/-	Growth, IC	0/3	0/3
19	M	70	Hepatitis C	Cirrhosis	NA	2,2	pT2G2, V-	+/+	Growth	0/3	0/3
20	F	61	Hepatitis C	Cirrhosis	NA	2,3	pT1G2, V-	+/-	Growth	0/3	0/3
21	M	51	Hepatitis C	Cirrhosis	NA	2,5	pT1G2, V-	+/-	Growth, IC	0/3	0/3
22	M	48	Hepatitis B	Fibrosis periportal and septal	NA	2,6	pT1G1, V-	+/-	Growth, IC, Mol	2/3	0/3
23	M	60	Hepatitis B	Cirrhosis and steatosis 5%	NA	3,2	pT2G2, V+	+/-	Growth, IC	2/2	0/2

^a CTNNB1- β-catenin gene, ^b TP53- tumor protein 53, ^c IC- immunohistochemistry, ^d Mol- molecular findings, ^e M- male, ^f F- female, ^g V–vascular invasion, NA-not available

Table 2: Intratumoral Heterogeneity Of Immune Phenotypes Per Tumor

<i>Analyzed tumor regions in large HCC 5-18cm (Ø10cm)</i>						
Pt	GS+	β-cat+	CK 7+	CD 44+	AFP+	EpCam+
1	6/6	4/6	4/6	6/6	0/6	0/6
2	3/9	3/9	4/9	0/9	0/9	0/9
3	0/6	0/6	2/6	0/6	3/6	4/6
4	4/6	6/6	0/6	3/6	1/6	0/6
5	0/3	0/3	0/3	3/3	0/3	0/3
6	0/10	0/10	6/10	7/10	0/10	0/10
7	3/8	0/8	0/8	8/8	2/8	0/8
8	0/7	0/7	0/7	0/7	7/7	0/7
9	0/3	0/3	3/3	3/3	0/3	0/3
10	6/6	0/6	3/6	0/6	0/6	0/6
11	0/7	0/7	4/7	6/7	3/7	0/7
12	0/7	0/7	0/7	0/7	0/7	0/7
13	7/10	7/10	1/10	0/10	0/10	0/10
14	0/5	0/5	3/5	3/5	5/5	5/5
<i>Analyzed tumor regions in smaller HCC 0.5-4cm (Ø2cm)</i>						
Pt	GS+	β-cat+	CK 7+	CD 44+	AFP+	EpCam+
15	0/3	0/3	3/3	0/3	0/3	0/3
16	0/3	0/3	0/3	0/3	3/3	0/3
17	0/3	0/3	3/3	0/3	0/3	0/3
18	1/3	0/3	2/3	0/3	0/3	0/3
19	0/3	0/3	3/3	0/3	0/3	0/3
20	0/3	3/3	0/3	3/3	0/3	0/3
21	1/3	1/3	1/3	0/3	0/3	0/3
22	2/3	3/3	2/3	3/3	0/3	0/3
23	2/3	2/3	0/3	0/3	0/3	0/3

Red: intratumoral heterogeneity of immune phenotypes in analyzed tumor regions,
 Green: homogeneous positivity, Gray: negativity of indicated marker

Table 3: Associations Of CTNNB1 Mutations And TP53 Mutations With Morphology And Immunohistochemistry

	Areas with CTNNB1 mutations (n=22)			Areas with TP53 mutations (n=10)		
	Number of areas	OR	p-value	Number of areas	OR	p-value
Morphology						
Solid	8(36%)	0.45	0.10	4(40%)	0.58	0.52
Trabecular	4(18%)	0.69	0.78	3(30%)	1.46	0.69
Pseudoglandular	10(45%)	3.46	0.01	3(30%)	1.38	0.70
Clear cell aspect	2(9%)	1.86	0.61	0	0	1
Fatty change	2(9%)	0.88	1	0	0	0.59
Immunohistochemistry						
β-catenin nucl. +	14(64%)	9.68	0.00	6(60%)	5.67	0.01
GS +	20(91%)	55.3	0.00	4(40%)	1.69	0.47
CK7+	13(59%)	2.47	0.08	4(40%)	1.16	1
AFP+	0	0	0.01	1(10%)	0.42	0.68
CD44+	8(36%)	0.94	1	7(70%)	4.48	0.04
EpCam+	0	0	0.2	0	0	1

OR: Odds ratio; GS= glutamine synthetase; nucl.+ = nuclear positivity; p-values based on Fisher's exact test; percentages refer to the total number of CTNNB1/TP53 mutated tumor areas; the predominant growth pattern of each tumor area was used for the analysis, cytologic features (if present) were additionally recorded